



HAL
open science

Effects of in situ CO₂ enrichment on *Posidonia oceanica* epiphytic community composition and mineralogy

T. E. Cox, M. Nash, Frédéric Gazeau, M. Déniel, E. Legrand, S. Alliouane, P. Mahacek, A. Le Fur, Jean-Pierre Gattuso, Sophie Martin

► To cite this version:

T. E. Cox, M. Nash, Frédéric Gazeau, M. Déniel, E. Legrand, et al.. Effects of in situ CO₂ enrichment on *Posidonia oceanica* epiphytic community composition and mineralogy. *Marine Biology*, 2017, 164 (5), pp.103. 10.1007/s00227-017-3136-7 . hal-01520318

HAL Id: hal-01520318

<https://hal.sorbonne-universite.fr/hal-01520318>

Submitted on 10 May 2017

HAL is a multi-disciplinary open access archive for the deposit and dissemination of scientific research documents, whether they are published or not. The documents may come from teaching and research institutions in France or abroad, or from public or private research centers.

L'archive ouverte pluridisciplinaire **HAL**, est destinée au dépôt et à la diffusion de documents scientifiques de niveau recherche, publiés ou non, émanant des établissements d'enseignement et de recherche français ou étrangers, des laboratoires publics ou privés.

1 **Effects of *in situ* CO₂ enrichment on *Posidonia oceanica* epiphytic community**
2 **composition and mineralogy**

3
4 T. E. Cox^{1*}, M. Nash², F. Gazeau¹, M. Déniel^{3,4}, E. Legrand^{3,4}, S. Alliouane¹, P. Mahacek¹, A.
5 Le Fur¹, J.-P. Gattuso^{1,5}, S. Martin^{3,4}
6

7 ¹Sorbonne Universités, UPMC Univ Paris 06, CNRS-INSU,
8 Laboratoire d'Océanographie de Villefranche, 181 chemin du Lazaret, F-06230 Villefranche-sur-
9 mer, France

10 ²Research School of Physics, The Australian National University, Acton, Australian Capital
11 Territory 0200, Australia

12 ³CNRS, UMR 7144, Station Biologique de Roscoff, Place Georges Teissier, Roscoff Cedex
13 29688, France

14 ⁴Laboratoire Adaptation et Diversité en Milieu Marin, Sorbonne Universités, UPMC Univ. Paris
15 6, Station Biologique de Roscoff, Place Georges Teissier, Roscoff Cedex 29688, France

16 ⁵Institute for Sustainable Development and International Relations, Sciences Po, 27 rue
17 Saint Guillaume, F-75007 Paris, France
18

19 *Corresponding author: erincox@hawaii.edu

20 **Running page head:** *In situ* CO₂ enrichment on epiphytes

21 ABSTRACT: Alterations in seagrass epiphytic communities are expected under future ocean
22 acidification conditions, yet this hypothesis has been little tested *in situ*. A Free Ocean Carbon
23 Dioxide Enrichment (FOCE) system was used to lower pH by a ~ 0.3 unit offset within a
24 partially enclosed portion (1.7 m³) of a *Posidonia oceanica* meadow (11 m depth) between 21
25 June and 3 November 2014. Leaf epiphytic community composition (% cover) and bulk
26 epiphytic mineralogy were compared every four weeks within three treatments, located in the
27 same meadow: a pH-manipulated (experimental enclosure) and a control enclosure, as well as a
28 nearby ambient area. Percent coverage of invertebrate calcifiers and crustose coralline algae
29 (CCA) did not appear to be affected by the lowered pH. Furthermore, fleshy algae did not
30 proliferate at lowered pH. Only Foraminifera, which covered less than 3% of leaf surfaces,
31 declined in manner consistent with ocean acidification predictions. Bulk epiphytic magnesium
32 carbonate composition was similar between treatments and percentage of magnesium appeared

33 to increase from summer to autumn. CCA did not exhibit any visible skeleton dissolution or
34 mineral alteration at lowered pH and carbonate saturation state. Negative impacts from ocean
35 acidification on *P. oceanica* epiphytic communities were smaller than expected. Epiphytic
36 calcifiers were possibly protected from the pH treatment due to host plant photosynthesis inside
37 the enclosure where water flow is slowed. The more positive outcome than expected suggests
38 that calcareous members of epiphytic communities may find refuge in some conditions and be
39 resilient to environmentally-relevant changes in carbonate chemistry.

40

41 **KEY WORDS:** ocean acidification, seagrass–epiphyte interactions, calcifiers, magnesium
42 carbonate, coralline algae, Bryozoa, pH, remineralisation

43

44 **Introduction**

45 Seagrass leaves and rhizomes are colonized by taxonomically diverse animal and algal
46 representatives referred to as epiphytes following the definition of Steel and Wilson (2003).
47 Seagrass and epiphytes form meadows which are highly valued for the services they provide
48 (Hemminga and Duarte 2000). For example, they play a fundamental role in maintaining
49 populations of exploited fisheries (Jackson et al. 2015). In the Mediterranean Sea, the seagrass
50 *Posidonia oceanica* L. (Delile) covers 23% of shallow water substratum (< 50 m, Pasqualini et
51 al. 1998) and leaf epiphytes can constitute ~30% of the canopy biomass (Prado et al. 2008).
52 Seagrass leaf epiphytes include coralline and filamentous algae, polychaetes, foraminiferans, and
53 bryozoans (Borowitzka et al. 2006). Among these groups are several calcifiers (e.g. coralline
54 algae, foraminiferans, serpulid polychaetes and some bryozoans) which contribute to carbonate
55 cycling (Frankovich and Zieman 1994; Perry and Beavington-Penney 2005). Moreover, *P.*

56 *oceanica* epiphytes can contribute 20 and 60% to meadow primary production and nutrient
57 uptake (Borowitzka et al. 2006; Lepoint et al. 2007). Most herbivores feed on algal epiphytes and
58 several grazers feed on the epiphytic invertebrates (Lepoint et al. 2000). As evidence of their
59 importance as a food source, epiphyte abundance and herbivore dynamics are tightly coupled
60 (Tomas et al. 2005).

61 Through the process of ocean acidification, the pH in the ocean is being lowered with a
62 subsequent decline in the proportion of carbonate ions (CO_3^{2-}) and an increase in the proportions
63 of bicarbonate ions (HCO_3^-) and dissolved carbon dioxide (CO_2). Surface ocean pH decreased by
64 0.1 units since the pre-industrial era and an additional 0.07 to 0.33 units decrease is expected by
65 2100 (Gattuso et al. 2015). The decline in the CO_3^{2-} concentration is projected to affect the
66 ability of calcifying organisms to maintain their skeletons (Feely 2004; Kroeker et al. 2013).
67 Macroalgal species can also respond differently to the increased carbon available for
68 photosynthesis and many, without calcified surfaces, are thought to be better competitors under
69 future ocean acidification conditions (Beer and Koch 1996; Koch et al. 2013). The concern is
70 changes in competitive abilities may cause shifts in composition at the community level (Fabry
71 et al. 2008; Kroeker et al. 2012; Gaylord et al. 2015; Sunday et al. 2017).

72 Seagrass epiphytic coverage and composition examined under lower pH conditions near
73 CO_2 vents and in the laboratory generally support future ocean predictions based upon
74 physiology and mineralogy. The epiphytic calcified community, which is often dominated by
75 crustose coralline algae (CCA), is less abundant at lowered pH. Furthermore, epiphytic
76 invertebrates with lower Mg content and those organisms that lack calcified skeletons, such as
77 filamentous algae, often persist at lowest pH conditions (Martin et al. 2008; Campbell and
78 Fourqurean 2014; Donnarumma et al. 2014; Cox et al. 2015). The predicted loss of CCA at

79 lowered pH is a global concern for ecosystem function. Species of CCA occur in temperate and
80 tropical seagrass beds and in a variety of other habitats (< 295 m depth) where they serve key
81 ecological roles (Littler and Littler 2013). They are known to be a food source, cement and
82 stabilize reefs, facilitate recruitment, and add significantly to sediments (Land 1970; Nelsen and
83 Ginsburg 1986; Littler and Littler 2013; Gischler et al. 2013). Although vent systems predict
84 their loss and shifts in the community under ocean acidification, they are not perfect predictors of
85 future ocean ecology owing to the large variability of pH in space and time (Hall-Spencer et al.
86 2008; Kerrison et al. 2011). Furthermore, laboratory experiments have difficulties accounting for
87 the many environmental variations and species interactions that can alter predicted outcomes
88 (e.g. Burnell et al. 2014). Therefore, predictions on the fate of *P. oceanica* meadows could
89 benefit from additional information provided by the manipulation of pH *in situ* on entire
90 communities for an extended period of time (months to years).

91 Alteration in the abundance of *P. oceanica* epiphytes will likely have repercussions to
92 meadow carbon cycling and feeding capacity. Therefore, the aim of the present study was to test
93 the hypothesis that *P. oceanica* epiphytic community will be impacted by ocean acidification.
94 We tested this hypothesis *in situ* with a Free Ocean Carbon Dioxide Enrichment (FOCE) system
95 (see Gattuso et al. 2014). This system allows pH to be manipulated continuously, in an
96 enclosure, at a fixed offset from ambient levels. The offset takes into account natural pH
97 fluctuations that may alter organismal responses. During a 4 month-experimental period,
98 epiphytic coverage as well as carbonate mass was quantified on *Posidonia* leaves. Lastly, some
99 minerals in epiphytic calcified structures are more susceptible to dissolution and mineral changes
100 at elevated partial pressure of CO₂ (*p*CO₂) are not well understood. Therefore, we analyzed
101 epiphytic mineralogy throughout the duration of the study.

102

103 **Methods**

104 **Experimental setup and system function**

105 This study used the European FOCE (eFOCE) system which allows for the *in situ*
106 manipulation of pH in benthic enclosures as an offset from ambient pH (Gattuso et al. 2014). The
107 system was deployed in the Bay of Villefranche, approximately 300 m from the Laboratoire
108 d'Océanographie de Villefranche (NW Mediterranean Sea, France; 43°40.73'N, 07°19.39'E).

109 The study design consisted of two clear, 1.7 m³ (2 m long x 1 m width x 0.85 m tall)
110 perspex enclosures that enclosed a portion of a *P. oceanica* meadow. The enclosures were
111 located at 11 m depth and were placed approximately 1.5 m apart. The pH in one enclosure,
112 referred to as the experimental enclosure, was lowered by ~0.3 units as an offset from ambient
113 pH as measured on the total scale. This offset was based upon the business-as-usual
114 representative concentration pathway RCP8.5 following Ciais et al. (2013) and corresponded to a
115 mean (\pm SD) pH_T of 7.75 ± 0.13 and $p\text{CO}_2$ of $971 \pm 323 \mu\text{atm}$. In the second enclosure, the pH
116 was not manipulated and it served as a control. A third treatment consisted of an open fiberglass
117 frame of the same dimensions as the enclosure footprint (2 m²). It was placed nearby (3 m of the
118 experimental enclosure) and in the same meadow. It is referred to as a reference plot and was
119 used to account for any effects generated by the enclosure structure. True replication was not
120 logistically feasible. Replication was sacrificed to 1) control pH precisely within enclosures of a
121 large enough size to contain *P. oceanica* and 2) sense pH and other aspects of the environment
122 continuously in the three treatment locations.

123 The details of the eFOCE system function and maintenance are described in Cox et al.
124 (2016) and a schematic can be found in Supplemental Figure 1 (Fig. S1). Briefly, the pH in the

125 experimental enclosure was altered using surface supplied seawater pumped into a mixing tank,
126 which was located on a surface platform. Pure CO₂ was bubbled into the mixing tank and the
127 resulting low pH seawater was pumped (flow rate up to 0.12 L min⁻¹), via tubing, underwater to
128 the proximity of the benthic enclosures. Prior to entering the enclosures, low pH (pH_T ~ 5.5) and
129 ambient seawater were mixed in an underwater tube and a set (x3) of centrifugal pumps (6.7 L
130 min⁻¹ each) injected ambient seawater in the control enclosure and lowered-pH seawater in the
131 experimental enclosure. Seawater pH was measured before entering the enclosures enabling the
132 automated adjustment of the low pH seawater injection to maintain the desired pH offset.
133 Seawater inside enclosures was circulated by a set of centrifugal pumps (4 per chamber; 6.7 L
134 min⁻¹ each) and exited through two openings (12 cm diameter). The renewal time of seawater in
135 each enclosure was ca. 1.5 h. The system contained a number of sensors: 4 potentiometric
136 Seabird 18-S pH sensors located inside each enclosure and in each mixing tube and three Seabird
137 37 SMP-ODO CTD with SBE 63 O₂ optodes and three LI-COR-192 PAR (photosynthetic active
138 radiation) sensors located in each enclosure and one nearby the enclosures (in ambient). The
139 carbonate chemistry within each treatment was determined at high frequency using average total
140 alkalinity together with sensed temperature, salinity and pH_T, in the R package, seacarb (see Cox
141 et al. 2016 for more details).

142 **Timeline**

143 The experiment comprised three periods in 2014: (1) the pre-acidification period, before
144 pH was manipulated, from 15 May to 11 June, (2) the transition period from 12 to 21 June, when
145 pH in the experimental enclosure was slowly lowered by no more than 0.05 units per day until an
146 offset of approximately -0.3 units was reached and (3) the experimental period from 22 June to 3
147 November when pH in the experimental enclosure was maintained at a offset of ~ -0.3 units.

148 **Collection of seagrass leaves**

149 Six to ten oldest leaf blades were collected from separate *P. oceanica* shoots growing
150 within the reference plot and enclosures. Oldest leaf blades, or the outer most leaf in the bundle,
151 were selected because these blades have more developed epiphytic communities (Cebrián et al.
152 1999). Divers collected intact leaves spaced evenly throughout the plot or enclosure at
153 approximately four week intervals during the acidification period in 2014, at time (T) 1 to 4: T1
154 occurred on 31 July, 39 d after acidification, T2 occurred on 4 September, 74 d after
155 acidification, T3 on 9 October after 109 d of acidification and T4 occurred on 10 November after
156 135 d of acidification. It should be noted that the acidification of the experimental enclosure
157 ended on 4 November 2014 but due to logistical constraints the final collection of blades were
158 made six days later. A set of ten leaves was also collected immediately after the transition period,
159 on 26 June 2014 (referred to as sampling interval, T0). These leaves were collected in a 2 x 1 m
160 area in the meadow, located ~2 m from the enclosures. They were collected outside the
161 enclosures and the reference plot to limit destructive sampling within the experimental setup but
162 still obtain a baseline measure. All leaves were collected above the sheath, placed into separate
163 plastic bags, transferred into a darkened cooler, and transported to the laboratory.

164 **Determination of epiphytic coverage and composition**

165 Leaves used for determination of epiphytic coverage and composition were kept in a
166 temperature controlled (20 to 22 °C), darkened room for less than 24 h until scanning was
167 completed. A high-resolution scanner *ZooScan* (Hydroptic, France; Gorsky et al. 2010) produced
168 colour images (2400 dpi) of leaves and their epiphytes. Five to seven images of leaves were used
169 to represent the assemblage within the reference plot and enclosures at each interval, except at
170 T1 when error resulted in three to four scanned leaf images being used per treatment.

171 The cell counter plug-in, in ImageJ, generated a grid (0.1 cm x 0.1 cm) superimposed on
172 the scanned image of the leaf. Organisms that occurred directly underneath each intersection of
173 the grid or point (231 to 1244 depending upon leaf length) were identified to the lowest possible
174 taxonomic or functional unit and counted. Fifteen lowest possible taxonomic or functional
175 groups were identified. These 15 were lumped into 11 groups that shared functional or
176 taxonomic similarity (see Table S3). The 11 groups were as follows: CCA (pigmented if pink in
177 coloration or bleached if thallus appeared white), non-calcified algae, Bryozoa, serpulid
178 polychaetes, Foraminifera, Hydrozoa, Porifera, unidentified, biofilm and ascidians. Biofilm was
179 defined as a group of microscopic organisms that formed a visible film across the surface of the
180 leaf. SEM images indicated this group is likely composed of diatoms and bacterial films and rod
181 forms. Percent cover by organism (or unit) was determined for each leaf by dividing the
182 organism intersections by the total number of intersections analysed and multiplying by 100.

183 **Calcium carbonate mass**

184 After scanning, the mass of CaCO_3 contained in the epiphytes was assessed using the
185 weight loss after acidification method (Bosence 1989; Perry and Beavington-Penney 2005).
186 Leaves with epiphytes were dried at 60 °C for 12 h, weighed (*A*, 0.01 mg), acidified with 5%
187 HCl, rinsed twice with deionised water, dried again at 60 °C for 12 h and re-weighed (*B*). Ten
188 young leaves without epiphytes were treated in the same manner (*C*). The weight of the epiphytic
189 calcareous mass was then determined from the following equation, $A - [B / (1 - C)]$.

190 **Determination of mineralogy**

191 After each leaf collection, three leaves from each treatment were set aside to air-dry (~22
192 °C) at room temperature. Dried epiphytes were gently scraped from separate leaves and ground
193 into a fine powder for X-ray diffraction (XRD, N = 3 per treatment). Additionally, to obtain a

194 baseline mineral profile the XRD analysis was performed on separate Bryozoa and CCA
195 sampled at T0 and carefully removed from the leaves and ground. Scanning electron
196 microscopy-energy dispersive spectroscopy (SEM-EDS) was further used to understand how the
197 minerals identified by XRD, were present on the leaf surface. Using SEM-EDS we compared the
198 skeletal structure of CCA between treatments.

199 XRD was carried out using a SIEMENS D501 Bragg-Brentano diffractometer equipped
200 with a graphite monochromator and scintillation detector, using $\text{CuK}\alpha$ radiation. Settings were a
201 step size of 0.02° and a scan speed of 1° per minute. Precision for determination of Mg-content
202 of Mg-calcite was $\sim 0.5\%$. Scan interpretation followed procedures described in Nash et al.
203 (2014). SEM-EDS was done using a Zeiss UltraPlus field emission scanning electron
204 microscope, equipped with an Oxford Inca EDS. For EDS measurements, the Zeiss was set to
205 15.0 kV, 15 mm working distance with a beam interaction volume ca. $3\ \mu\text{m}$. Imaging was at
206 3 mm working distance and 3 kV. Samples were platinum coated. A sample was embedded in
207 crystal bond and polished for precise SEM-EDS measurements or mounted intact and attached
208 using carbon tape. Aragonite was quantified using the area under the curve method (Diaz-Pulido
209 et al. 2014). Many Mg-calcite peaks had minor asymmetry on the lower 2-theta side indicating
210 the presence of small amounts of calcite. Comparisons of relative calcite asymmetry were made
211 using the principles of peak asymmetry developed in Nash et al. (2014).

212 **Statistical analyses**

213 The approach used was to monitor the epiphytic community at three sites: control
214 enclosure, experimental enclosure, and a reference plot. This study, similar to many natural
215 experiments, lacks true replication (Hurlbert 1984). In unreplicated designs in ecology, the
216 emphasis is on the estimation of effect size and the unique ecological perspective provided

217 (Hurlbert 1984; Stewart-Oaten et al. 1986; Oksanen 2001; Davies and Gray 2015). Inferential
218 statistics were avoided. Furthermore, a large effect size was expected based upon previous study
219 results (e.g. Martin et al. 2008).

220 Multivariate analyses were used to compare the leaf epiphytic communities. Prior to
221 analyses, the epiphytic coverage at each interval was averaged. Thus, there was one value for
222 each of the three treatments (reference, control enclosure, and the experimental enclosure) at
223 each interval (T1-T4). A square root transformation was applied and a Bray-Curtis resemblance
224 matrix created between each interval-treatment assemblage (4 intervals x 3 treatments = 12 leaf
225 assemblages). Dissimilarities were visualized with an nMDS (non-metric multi-dimensional
226 scaling) plot. A two-way (treatment x interval) Analysis of Similarity (ANOSIM) without
227 replication and 999 permutations was used to examine for differences. This is a valid approach in
228 ecological monitoring when there is pseudoreplication (Clarke 1993). The global R from an
229 ANOSIM indicates effect size. It ranges from -1 to 1 and is analogous to a correlation
230 coefficient; a value close to zero indicates no or little distinction between a prior groups. The
231 ANOSIM was followed by two separate (treatment and interval) similarity percentage analyses
232 (SIMPER) to identify the amount each taxonomic or functional group contributed to
233 dissimilarity.

234 Data from leaves collected at T0 (before the perturbation) were not used in multivariate
235 analyses because they were only collected at one instance and outside the experimental setup.
236 Similarly, organisms that occurred on one to three leaves out of 70 were removed prior to
237 analyses to eliminate their inflated influence on dissimilarities.

238 The abundance (mean, median, and range) of specific taxa, CaCO₃ mass, and epiphytic
239 mineral composition were compared qualitatively through time between the three treatments;

240 paying careful attention to any directional deviations observed on leaves from the experimental
241 enclosure.

242 **Results**

243 **Environmental and experimental conditions**

244 Environmental and experimental conditions as well as seagrass growth are fully
245 described in Cox et al. (2016). There were 150 to 175 shoots m⁻² of *P. oceanica* inside each plot
246 and enclosure and few other macrophytes (< 11% coverage). Leaf biometrics were not affected
247 by the lowered pH. Average shoot height increased from 40.6 cm in April to 73.4 cm in August
248 then declined to 24.8 cm in November.

249 The carbonate chemistry is summarized in Table 1 and the diel variability is provided in
250 Table S1. The pH_T in the meadow (ambient) ranged from a monthly mean of 7.98 (± 0.06 SD) to
251 8.11 (± 0.04 SD, Table 1). The mean saturation states of aragonite (Ω_a) and calcite (Ω_c) ranged
252 from 3.1 to 3.6 and 4.9 to 5.4 from June to September, respectively. The diel pH_T change
253 differed among months from 0.04 to 0.12. It corresponded to the daily change in CO₂
254 concentration driven by community primary production, respiration and calcification.

255 The carbonate chemistry in the control enclosure and the ambient environment were
256 similar (monthly mean differed ≤ 0.06 units). The diel change in pH_T within the control
257 enclosure was slightly greater than in ambient and was consistent in the pre- and during
258 acidification period (median ± median absolute deviation 0.14 ± 0.06 and 0.14 ± 0.06).

259 During the acidification period, the pH in the experimental enclosure was maintained at a
260 mean -0.26 unit offset (monthly mean values from -0.22 to -0.29 pH units) from the control
261 enclosure (Table S1). Monthly mean values of saturation state with respect to aragonite (Ω_a)
262 ranged from 2.0 (± 0.05 SD) in October to a high of 2.5 (± 0.06 SD) in August and saturation

263 state with respect to calcite (Ω_c) ranged from 3.0 (± 0.07 to 0.008 SD) in September and October
264 to 3.8 (± 0.09 SD) in August. Median diel pH range in the experimental enclosure was two to
265 three times larger than the control (monthly ranged from 0.09 to 0.29 pH units) and had greater
266 variability. Variation was attributed to lowered buffering capacity of seawater with lowered pH.

267 Monthly differences as summarized in Cox et al. (2016) were evident, particularly for
268 temperature (mean monthly range: 17.7 to 24.2°C) and PAR (mean monthly range: 1.3 to 7.3
269 mol photons $m^{-2} d^{-1}$, Table S2) but were similar in the ambient, control and experimental
270 enclosures.

271 **Leaf epiphytic community description**

272 Overall, CCA were the most dominant epiphyte occurring on all leaves at coverages
273 between 0.8 to 58.8%, followed by the lesser abundant biofilm (0 to 22.0%) and Bryozoa (0 to
274 20.8 %). Hydroids and sponges were found on 3 of the 70 leaves (< 2%). An ascidian occurred at
275 12% on one leaf collected from the reference plot.

276 SEM images confirmed the presence of CCA, Bryozoa, Foraminifera, serpulid
277 polychaetes and biofilm. At this increased SEM resolution, bacterial films, rod structures and
278 diatoms were visually distinguishable. These organismal groups were likely undetected or
279 grouped to ‘biofilm’ in the quantification of macroepiphytes. Unidentified rod structures of 1-2
280 μm in length were commonly found on the epiphytes but not directly on the leaves (Fig. S2).
281 Diatoms were observed both on epiphytes and leaf surfaces.

282 **Spatial and temporal patterns in epiphytic community**

283 There was little distinction in epiphytic composition and coverage found on leaves from
284 the enclosures and reference plot yet, clear differences were observed between T1-T4 intervals

285 (ANOSIM: treatment, global R = 0.25, p-value = 0.28; interval, global R = 0.56, p -value =
286 0.003; Fig. 1)

287 Indeed, SIMPER routine indentified dissimilarities (TS4) between communities in the
288 plot and enclosures to be small (ranged from 19.2 to 26.7%). Differences in abundances of
289 biofilm and pigmented CCA contributed most (Table S4, 19.1 to 33.3%) to treatment
290 dissimilarities. Leaves from the reference plot had an overall (across all sampling intervals, n =
291 18 to 20 leaves) greater coverage of pigmented CCA (mean \pm SD, reference = 27.9 ± 15.3 ,
292 control = 19.5 ± 9.4 and experimental = $23.4 \pm 10.7\%$) and leaves from the control had a greater
293 cover of biofilm (mean \pm SD, reference = 0.8 ± 0.9 , control = 7.2 ± 5.3 , experimental = $2.8 \pm$
294 2.5%). It was also noted that there was a greater coverage of biofilm in enclosure communities,
295 with percentages more similar to those observed at T0 in leaves from the ambient. In SEM
296 images, relatively greater numbers of diatoms were observed on leaves collected in the
297 enclosures than on leaves collected at T0 and in the reference plot.

298 Dissimilarity in communities increased with increasing duration between sampling
299 intervals. For example, the overall (combined treatments) community at T1 was most dissimilar
300 from communities at T3 and T4 (20.9 to 30.2% dissimilar, respectively) and least dissimilar from
301 the community at T2 (14.1%). Also, the community at T2 was more similar to the community at
302 T3 than the community at T4 (Table S5, T2 and T3 were 18.2% dissimilar, T2 and T4 were
303 26.7% dissimilar).

304 In enclosures and in the reference plot, there was a decline in the abundance of CCA
305 (bleached and pigmented, separate groups in analyses) from July (mean \pm SD, T1 $31.4 \pm 8.3\%$)
306 to November (mean \pm SD, T4 $11.7 \pm 6.2\%$). Bleached and healthy appearing CCA showed
307 similar trends in time. Together, they accounted for 33 to 55% of the dissimilarity between

308 intervals. Other epiphytic groups also declined from T1 to T4 and contributed to interval
309 dissimilarities (each contributed between 4.1 to 13.7%), these included non-calcified algae (mean
310 \pm SD, T1 $2.2 \pm 2.7\%$ to T4 $0.3 \pm 0.4\%$) and Bryozoa (mean \pm SD, T1 $2.1 \pm 1.4\%$ to T4 $0.5 \pm$
311 0.6%).

312 The abundances of epiphytes found on the T0 leaves ($n = 7$, collected from nearby
313 enclosures before the perturbation), highlight the large spatial or temporal variability in
314 abundance of some groups, such as Bryozoa and Foraminifera (Fig 2).

315 **Trends in organismal coverage to evaluate predicted pH effects**

316 Overall (pooled across sampling intervals), leaves from the experimental enclosure had a
317 slightly greater mean coverage of pigmented CCA than those from the control enclosure (Fig. 2
318 A) and the range of coverage often overlapped. The coverage of non-calcified algae (Fig. 2D,
319 mostly *Dictyota* sp.) declined in all treatments and the overall mean (\pm SD) was slightly lower in
320 the experimental than in the control enclosure ($1.2 \pm 1.8\%$ vs $0.7 \pm 0.7\%$). It contributed 4.7% to
321 enclosure differences. Leaves from the experimental enclosure also tended to have a relatively
322 greater coverage of invertebrate calcifiers (Fig. 2E, F; mean \pm SD, control *versus* experimental,
323 Bryozoa: $0.6 \pm 0.8\%$ vs $1.0 \pm 0.9\%$; serpulid polychaetes: $0.1 \pm 0.1\%$, vs $0.4 \pm 0.4\%$). These
324 abundances contributed 8% each to differences between enclosures. Only, leaf epiphytic
325 Foraminifera (Fig. 2G) had a directional change in abundance distinct from the change in
326 abundances on leaves from the control enclosure and reference plot. Foraminifera coverage was
327 greatest on leaves at T1 within the experimental enclosure (0 to 1%), they declined at T2 (0 to
328 0.1%) and disappeared from the collected leaves at T3 and T4. However, this taxon is rare
329 (indicated by low coverage, $<1\%$) and coverage between leaves can be highly variable (see T0).
330 It contributes 7% to enclosure community differences (Table S4).

331 **Calcium carbonate mass**

332 CaCO_3 mass on leaves ranged from 8.6 to 24.7 mg cm⁻² (Fig. 3). There were no clear
333 consistent patterns that would indicate seasonal changes or lowered pH effect.

334 **Mineralogy**

335 The magnesium carbonate composition of leaf epiphytes ranged from 10.6 to 13.2 mol%
336 MgCO_3 and there was no indication of a low pH effect (Fig. 4). The mean (\pm SD) mol % MgCO_3
337 was 11.9 ± 0.6 on leaves from the reference plot, 12.1 ± 0.9 on leaves from the control and 12.0
338 ± 0.7 on leaves from the experimental enclosure. Values obtained on samples collected at T0
339 confirmed that CCA and Bryozoa were, respectively, 11.3 to 11.7 and 8.3 to 8.8 mol% MgCO_3 .

340 Changes in epiphytic mol% MgCO_3 by sampling interval appeared to be seasonal (Fig.4).
341 The community mean (\pm SD) value tended to increase from T0 (June, 10.7 ± 0.1) to T1 (July,
342 11.1 ± 0.4) and maintained a similar composition between T2 and T4 (September to November,
343 12.2 ± 0.4 and 12.4 ± 0.6 mol% MgCO_3).

344 There were two other mineral phases present in the epiphyte community in addition to
345 magnesium calcite, calcite and aragonite. Aragonite was present on all 24 leaves examined from
346 the enclosures but was not present on leaves collected from the reference plot, nor from T0
347 leaves from the ambient environment (16 leaves in total). The proportion of aragonite in bulk
348 epiphytes between enclosures was similar at each interval from T1 to T3. At T4, it was greater in
349 two of the three epiphyte samples collected from the control enclosure and in three of three
350 samples collected from the experimental enclosure (Fig. 4).

351 Calcite was predominantly present in epiphytes collected from the reference plot and at
352 T0 in ambient epiphytes (Fig. 4). Epiphytes from the ambient environment at T0 and T1 to T3 in
353 the reference plot had minor calcite amounts present as indicated by slight asymmetry of the Mg-

354 calcite peak. There were separate peaks for calcite and Mg-calcite for bulk epiphytes at T4,
355 indicating substantial amounts present, but they were not quantified. The asymmetry method is
356 not appropriate when the peaks are entirely separate, as for the T4 samples. In this case the value
357 of (-) 6 was given, being the approximate difference between the value for calcite (which
358 contains ~3-4 mol% MgCO₃) and Mg-calcite (9-10 mol% MgCO₃).

359 SEM-EDS was used to visualize the surfaces of leaf epiphytes and examine the location
360 of mineral phases. Imaging was undertaken on subsamples from three leaves collected at T0
361 from the ambient environment and from both enclosures and reference plot at T1 and T4. Loose
362 grains of Mg-calcite were present on the seagrass surface (Fig. S3). These appeared to be
363 remnant grains after the surficial CCA had broken off, possibly during sample preparation.
364 Calcification features of the CCA from the enclosures and reference plot appeared similar in
365 structure (Fig. 5). There were not any structural indications of dissolution from the lowered pH.
366 EDS measurements also confirmed that the CCA were Mg-calcite.

367 All the imaged CCA had areas of alteration where their cellular structure was no longer
368 intact (Fig. 6). EDS measurements showed that alteration areas were responsible for the calcite
369 or aragonite identified by XRD. Altered surfaces of epiphytic CCA revealed different mineral
370 phases related to a “structural effect” from the enclosures. On leaves from the ambient
371 environment (reference plot as well as T0), the altered CCA surfaces appeared rough and were
372 composed of calcite with no micro-endoliths visible. In contrast, the altered surfaces of CCA on
373 leaves from the enclosures were aragonitic. The aragonite-altered CCA showed areas that
374 appeared similar to the calcitic altered areas on CCA from the ambient, with the exception that
375 there were also partially eroded cells that had altered to aragonite (Fig. 6, Fig. S4). Crystal
376 morphology of the aragonite varied from blocky to typical aragonite needle shape. Particular

377 attention was paid to the November samples from the reference plot to determine whether there
378 were other epiphytes or changes that could be responsible for the substantially greater amount of
379 calcite observed relative to the amount observed at T0 and T1 in the epiphytes grown in the
380 ambient environment. The only calcite detected was in alteration areas that appeared similar to
381 that observed previously at T0 and T1. Diatoms and bacterial films were observed on the
382 surfaces of leaves and CCA, often in close proximity to the altered algal surfaces (Fig. S4).

383 **Discussion**

384 The lack of a pH effect on *P. oceanica* epiphytic community is in contrast with findings
385 from previous laboratory manipulations and observations of communities conducted near CO₂
386 vents where the pH is naturally lower (Hall-Spencer et al. 2008; Martin et al. 2008;
387 Donnarumma et al. 2014; Cox et al. 2015). Martin et al. (2008) showed a complete
388 disappearance of epiphytic coralline algae and the persistence of bryozoans at an average pH_T of
389 7.7, but with large temporal variations from < 7.0 to > 8.1. Donnarumma et al. (2014), at the
390 same CO₂ seep, showed that the calcifying species tend to be less competitive as pH_T decreases
391 (8.1 to 6.7) and that leaves were dominated by filamentous algae, hydroids and tunicates at the
392 lowest pH_T (mean 6.7). In the laboratory, Cox et al. (2015) exposed *P. oceanica* shoots with their
393 associated epiphytes to three constant pH levels (pH_T 8.1 ambient, 7.7 and 7.3) for four weeks.
394 Under both low pH treatments, there was a reduction of CCA and reduced calcification rates.
395 Similar shifts in community composition have been noted on other seagrass species as a
396 consequence of lowered pH (Burnell et al. 2014; Campbell and Fourqurean 2014; Martínez-
397 Crego et al. 2014).

398 In the present study, the epiphytic community was largely composed of CCA and
399 Bryozoa. A similar proportion of epiflora to epifauna composition on *P. oceanica* has been

400 described in other investigations (Lepoint et al. 1999; Martin et al. 2008; Prado et al. 2008; Cox
401 et al. 2015) and coverages were similar to those reported by Cox et al. (2015) and Prado et al.
402 (2008). The decline in coverage at T4 coincides with the period of known decline of seagrass
403 biomass and leaf turnover after storm events in the autumn (Alcoverro et al. 1995).

404 CCA are often identified as having a large susceptibility to ocean acidification (Nelson
405 2009; Koch et al. 2013; Hofmann and Bischof 2014; McCoy and Kamenos 2015). CCA
406 epiphytes on *P. oceanica* have exhibited lowered calcification rates and coverage near and below
407 the pH_T of 7.7 (Martin et al. 2008; Cox et al. 2015). Martin et al. (2008) has also demonstrated
408 their vulnerability to dissolution at pH_T of 7.0 with strong undersaturation of carbonate.
409 Although some species are able to reduce carbonate demands by altering their structural
410 thickness (McCoy and Ragazzola 2014), we did not observe any visible or quantifiable alteration
411 in CCA skeletons related to pH manipulation, even after four months of exposure.

412 Bryozoa have also been studied in the vicinity of CO_2 vents as well as in the laboratory
413 (Rodolfo-Metalpa et al. 2010; Lombardi et al. 2011b; Lombardi et al. 2011a; Smith 2014). Many
414 have an outer cuticle beneath which the mineralized skeleton forms. The protective cuticle
415 barrier and low Mg-calcite composition or ability to alter mineral composition has been used to
416 explain their persistence on leaves at volcanic CO_2 seeps with a pH_T as low as 6.98 (Martin et al.
417 2008; Rodolfo-Metalpa et al. 2010; Donnarumma et al. 2014). Transplant experiments, however,
418 indicate that some group members can be negatively affected (decreased thickness and signs of
419 dissolution) by ocean acidification particularly in warmer months (Rodolfo-Metalpa et al. 2010;
420 Lombardi et al. 2011b; Lombardi et al. 2011a). Therefore, it appears that the pH environment in
421 the experimental enclosure, even during the warmer months, was not detrimental to calcification
422 for the bulk of the community.

423 It should be noted that despite rarity, Foraminifera did decline in the experimental
424 enclosure in a pattern consistent with a response to ocean acidification. This observation is in
425 agreement with 20 out of 26 studies reviewed on Foraminifera under elevated $p\text{CO}_2$ that have
426 reported negative responses to lowered pH (Keul et al. 2013).

427 Recently, there have been several studies with outcomes which conflict or fail to support
428 widely-held ocean acidification projections. For example, Martin and Gattuso (2009), and
429 Egilisdottir et al. (2013) describe no clear effect of minimally lowered pH on calcifiers. Even for
430 epiphytes, Apostolaki et al. (2014) and Saderne and Wahl (2013) did not find a loss in calcified
431 coverage or reduced calcification rates at lowered pH. The present study outcome adds to the
432 growing literature which suggests that calcified communities in their natural settings can be little
433 affected by minimal changes in surrounding carbonate chemistry.

434 There have been many speculations on the conditions that result in conflicting outcomes
435 for calcifiers under lowered pH. Discrepancies are attributed to species specificity, other
436 environmental conditions that stress or limit organismal physiology (e.g. differences in light,
437 temperature, or combined stressors), or limitations and differences in study design (e.g. treatment
438 levels used, Kroeker et al. 2010; Koch et al. 2013; Gazeau et al. 2013).

439 Some macroalgae and benthic invertebrates are known to respond differently to pH
440 fluctuations than they do to a mean pH difference (Britton et al. 2016; Small et al. 2016). The
441 median diel pH variation was 0.1 in the ambient meadow. The median diel pH range in the
442 experimental enclosure was two to three times larger than the control (0.09 to 0.29 pH units).
443 This difference could not be explained by O_2 fluxes alone and instead was attributed to lowered
444 buffering capacity of seawater with lowered pH (Cox et al. 2016). Because of natural pH
445 fluctuations, it is hypothesized that organisms in seagrass meadows may already experience and

446 be pre-adapted to pH levels projected into the next century (Hendriks et al. 2014a). In the present
447 study, the 0.1 diel pH variability in the meadow would not support possible acclimation to a pH_T
448 of 7.7. Productivity of coastal macrophytes can buffer the impacts of ocean acidification by
449 providing a daily window of maximum $CaCO_3$ saturation where calcification can be more
450 efficient (Anthony et al. 2011; Anthony et al. 2013; Hendriks et al. 2014b; Cornwall et al. 2015).
451 It is possible that the pH offset used could have allowed for buffering at the leaf blade surface
452 and prevented CCA loss. To limit an impact, however, buffering in daylight must offset the
453 lowered pH that surrounds the community in the absence of photosynthesis at night. For
454 sensitive taxa the benefit of pH fluctuations appears limited (Cornwall et al. 2014; Johnson et al.
455 2014; Roleda et al. 2015). For instance, in the laboratory recruits of coralline algae had relatively
456 lowered growth rates when pH fluctuated as opposed to when pH was constant and lowest
457 growth occurred when pH fluctuations were altered to mimic a future ocean acidification
458 scenario (-0.4 difference from ambient, Roleda et al. 2015). Adult coralline algae, often more
459 tolerant to ocean acidification conditions, were unaffected (Roleda et al. 2015). Congruent with
460 the reduced numbers observed in the present study with exposure to lower pH, algal surfaces did
461 not provide refugia for foraminifera assemblages along a gradient of overlying seawater
462 acidification in Levante Bay, Italy (Pettit et al. 2015).

463 The outcome for epiphytes growing in host plant boundary layers may also depend upon
464 the pH scenario used. For example, recruitment and growth of calcifying serpulids and bryozoan
465 on the alga *Fucus serratus* were weakly to not affected at $pH_T = 7.7$ but were reduced at $pH_T =$
466 7.3 (Saderne and Wahl 2013). The ocean acidification scenario used (mean pH_T of 7.75) could
467 also explain the outcome in the present study. Maintaining a calcified skeleton presumably
468 becomes more difficult and costly as seawater gets closer to undersaturation (Kleypas et al.

469 1999). Seawater in the pH manipulated enclosure was lower than ambient yet, it remained
470 saturated with respect to both calcite and aragonite (3.6 and 2.2). CCA have the ability to raise
471 the pH within their boundary layer to limit the potential negative impacts of decreased ambient
472 pH when seawater is not undersaturated (Hofmann et al. 2016). In contrast, at CO₂ seeps, pH
473 near the vents can be highly variable and organisms can be exposed to pH levels substantially
474 lower than projections for the next century (Kerrison et al. 2011). In addition, organismal
475 physiological responses can be confounded by biological conditions facilitated by venting, not
476 related to lowered pH (Vizzini et al. 2013).

477 Enclosures, while circulated and partly open, likely slowed water motion and could
478 possibly account for the relative increase of diatoms and provided a better refuge for calcifiers.
479 Diatoms are ubiquitous members of seagrass microepiphytic communities (Borowitzka et al.
480 2006; Mabrouk et al. 2014). Pinckeney and Fiorenza (1998) reported increased prevalence of
481 diatoms on leaves in slower flows in the Atlantic. Microalgae were also more prominent on *P.*
482 *oceanica* which has a greater structural canopy that can slow water movement than on
483 *Cymodocea nodosa* (Mabrouk et al. 2014). Slowed water flows, like those that occur in dense
484 canopies, increase boundary layer thickness surrounding plants and potentially allow for greater
485 buffering capacity in daylight (Hurd 2015) and lower buffering capacity at night. Therefore, in
486 the eFOCE experiment, the structural barrier of the enclosure may have affected the response
487 both positively and negatively. The lack of effect on epiphytes suggest that the combined
488 response was balanced.

489 pH effects on communities are known to be altered by seasonal factors (Burnell et al.
490 2014; Baggini et al. 2014; Martínez-Crego et al. 2014), yet in a year-long study, at an area with
491 volcanic CO₂ seeps, epiphytic calcifier abundance on *P. oceanica* leaves was negatively

492 correlated with pH (Donnarumma et al. 2014). In contrast, the pH perturbation in the present
493 study occurred during a period with large seasonal environmental change (July to November)
494 and a climax epiphytic community, and no pH effects were observed. We also observed, in all
495 treatments, what appeared to be a recruitment event of filamentous algae and both CCA recruits
496 (small patches) and adults with reproductive conceptacles. Thus, we surmise that if the eFOCE
497 experiment was extended for a full year the outcome would be the same. Even though this
498 experiment was conducted in a period of biomass decline, we do not think it masked an impact.
499 In other studies, a decline in CCA calcification rates and coverage has occurred rapidly (weeks to
500 months), a time frame well within the duration of study and the sampling frequency. A repeated
501 experiment with extended experimental duration is needed to clarify long-term effects and to
502 include the period of peak faunal recruitment not captured in the current study.

503 To the best of our knowledge, this is the only study to concurrently investigate temporal
504 changes and pH effects on bulk epiphytic mineralogy. The only identifiable trend for Mg content
505 was over time. The increase in $MgCO_3$ after August (T2) could be explained by the seasonal
506 reduction in abundance of invertebrate calcifiers often composed of lower Mg-calcite.
507 Alternatively, or in combination, the incorporation of more Mg may be due the 2 to 6 °C increase
508 (e.g. Chave and Wheeler 1965; Diaz-Pulido et al. 2014) that occurred from June to August (T0 to
509 ~T2). The presence of calcite in the epiphytes from the reference plot, compared to its absence in
510 the epiphytes sampled in the enclosures, which instead had aragonite, is at this time without
511 explanation. Similarly, the increase in calcite and aragonite that occurred at T4 is without
512 explanation. There are many reports of aragonite in CCA (Nash et al. 2011; Smith et al. 2012;
513 Diaz-Pulido et al. 2014; Kraysky-Self et al. 2016). We are not aware of any report of calcite in
514 live CCA and thus this is the first documented alteration to calcite for CCA.

515 Accurate ecological projections of future oceans should arise as a consensus from
516 combined study approaches: observational, controlled laboratory, modeling, and *in situ*
517 experimentation. This study addressed a need for *in situ* pH manipulation to account for the
518 complexity in community response to ocean acidification. Additionally, the study design
519 accounted for natural pH variation that is often ignored when pH is manipulated *in situ*. While
520 large scale unreplicated experiments, like eFOCE, can provide valuable ecological information
521 they do have drawbacks (Hurlbert 1984; Oksanen 2001; Davies and Gray 2015). Replicated
522 enclosures were not feasible at this stage. Alternative hypotheses that we cannot robustly exclude
523 include (1) there were small pH effects difficult to quantify (2) that the conflicting outcome is
524 due to some ‘lurking’ variable. However, several recommended steps (Oksanen 2001; Davies
525 and Gray 2015) were taken to try to reduce erroneous conclusions that may occur including: (1)
526 care was taken to select study locations that were similar in depth and seagrass density to reduce
527 confounding variables (2) the environment was continuously monitored to ensure they were
528 similar to those in ambient, (3) repeated measurements were made at the same location through
529 time and compared to ‘before’ measurements when possible, (4) comparisons from the pH
530 manipulated enclosure were made to two different spatial locations and (5) statistics used did not
531 require replication.

532 The use of a FOCE system to study the epiphytic community on *P. oceanica* leaves
533 provides a more positive outlook on the future of meadows than the projections based largely on
534 observations near CO₂ vents. This conclusion should be tempered until more assessments are
535 conducted with greater replication under a variety of conditions found in meadows. Nevertheless,
536 results add to the growing evidence that calcareous members of macrophyte dominated
537 communities may be more resilient to minimal changes in carbonate chemistry.

538

539 **Acknowledgements** We would like to acknowledge the following people who assisted in the
540 laboratory, in the field, or with engineering: E. Beck Acain, J. Acain, J. Delille, L. van der
541 Heijden, M. Maillot, F. Moullec, S. Schenone, L. Urbini, K. Walzyńska. We are grateful to A.
542 Elineau for help with the ZooScan. We also thank J.-J. Pangrazi, R. Patix and E. Tanguy for
543 aide in construction of the enclosures. G. de Liege, D. Luquet and D. Robin kindly assisted in
544 diving collection activities. This work was funded by the ‘European Free Ocean Carbon
545 Enrichment’ (eFOCE; BNP-Paribas Foundation), the ‘European Project on Ocean Acidification’
546 (EPOCA; grant agreement 211384) and the MISTRALS-MERMEX (INSU, CNRS) program.

547

548 **Ethical Statement**

549 The authors declare that they have no conflict of interests and all applicable guidelines for the
550 use of animals were followed.

551 **References**

- 552 Alcoverro T, Duarte C, Romero J (1995) Annual growth dynamics of *Posidonia oceanica*:
553 contribution of large-scale versus local factors to seasonality. *Mar Ecol Prog Ser*
554 120:203–210. doi: 10.3354/meps120203
- 555 Anthony KRN, Diaz-Pulido G, Verlinden N, Tilbrook B, Andersson AJ (2013) Benthic buffers
556 and boosters of ocean acidification on coral reefs. *Biogeosciences* 10:4897–4909. doi:
557 10.5194/bg-10-4897-2013
- 558 Anthony KRN, Kleypas J, Gattuso J-P (2011) Coral reefs modify their seawater carbon
559 chemistry - implications for impacts of ocean acidification. *Global Change Biol* 17:3655–
560 3666. doi: 10.1111/j.1365-2486.2011.02510.x
- 561 Apostolaki ET, Vizzini S, Hendriks IE, Olsen YS (2014) Seagrass ecosystem response to long-
562 term high CO₂ in a Mediterranean volcanic vent. *Mar Environ Res* 99:9–15
- 563 Baggini C, Salomidi M, Voutsinas E, Bray L, Krasakopoulou E, Hall-Spencer JM (2014)
564 Seasonality affects macroalgal community response to increases in pCO₂. *PLoS ONE*
565 9:e106520. doi: 10.1371/journal.pone.0106520
- 566 Beer S, Koch E (1996) Photosynthesis of marine macroalgae and seagrasses in globally changing
567 CO₂ environments. *Mar Ecol Prog Ser* 141:199–204
- 568 Borowitzka MA, Lavery PS, van Keulen M (2006) Seagrasses: Biology, Ecology and
569 Conservation. In: Larkum AWD, Orth RJ, Duarte CM (eds) *Epiphytes of seagrasses*.
570 Springer, Dordrecht, The Netherlands, pp 441–461
- 571 Bosence D (1989) Biogenic carbonate production in Florida Bay. *Bull Mar Sci* 44:419–433
- 572 Britton D, Cornwall CE, Revill AT, Hurd C, Johnson C (2016) Ocean acidification reverses the
573 positive effects of seawater pH fluctuations on growth and photosynthesis of the habitat-
574 forming kelp, *Ecklonia radiata*. *Sci Rep*. doi: 10.1038/srep26036
- 575 Burnell O, Russell B, Irving A, Connell S (2014) Seagrass response to CO₂ contingent on
576 epiphytic algae: indirect effects can overwhelm direct effects. *Oecologia* 176:871–882
- 577 Campbell JE, Fourqurean JW (2014) Ocean acidification outweighs nutrient effects in
578 structuring seagrass epiphyte communities. *J Ecol* 102:730–737. doi: 10.1111/1365-
579 2745.12233
- 580 Cebrián J, Enríquez S, Fortes MD, Agawin N, Vermaat JE, Duarte CM (1999) Epiphyte accrual
581 on *Posidonia oceanica* (L.) Delile leaves: Implications for light absorption. *Bot Mar*
582 42:123–128. doi: 10.1515/BOT.1999.015
- 583 Chave KE, Wheeler BD (1965) Mineralogic changes during growth in the red alga,
584 *Clathromorphum compactum*. *Science* 147:621–621. doi: 10.1126/science.147.3658.621

- 585 Ciais P, Sabine C, Bala G, Bopp L, Brovkin V, Canadell J, Chhabra A, DeFries R, Galloway J,
586 Heimann M, Jones C, Le Quéré C, Myneni RB, Piao S, Thornton P (2013) Carbon and
587 other biogeochemical cycles. Cambridge University Press, Cambridge, United Kingdom
588 and New York, NY, USA
- 589 Clarke KR (1993) Non-parametric multivariate analyses of changes in community structure.
590 *Austral Ecol* 18:117–143. doi: 10.1111/j.1442-9993.1993.tb00438.x
- 591 Cornwall C, Pilditch C, Hepburn C, Hurd CL (2015) Canopy macroalgae influence understorey
592 corallines' metabolic control of near-surface pH and oxygen concentration. *Mar Ecol*
593 *Prog Ser* 525:81–95. doi: 10.3354/meps11190
- 594 Cornwall CE, Boyd PW, McGraw CM, Hepburn C, Pilditch CA, Morris JN, Smith AM, Hurd
595 CL (2014) Diffusion boundary layers ameliorate the negative effects of ocean
596 acidification on the temperate coralline macroalga *Arthrocardia corymbosa*. *PLoS ONE*
597 9:e97235. doi: 10.1371/journal.pone.0097235
- 598 Cox TE, Gazeau F, Alliouane S, Hendriks IE, Mahacek P, Le Fur A, Gattuso J-P (2016) Effects
599 of *in situ* CO₂ enrichment on structural characteristics, photosynthesis, and growth of the
600 Mediterranean seagrass *Posidonia oceanica*. *Biogeosciences* 13:2179–2194. doi:
601 10.5194/bg-13-2179-2016
- 602 Cox TE, Schenone S, Delille J, Díaz-Castañeda V, Alliouane S, Gattuso JP, Gazeau F (2015)
603 Effects of ocean acidification on *Posidonia oceanica* epiphytic community and shoot
604 productivity. *J Ecol* 103:1594–1609. doi: 10.1111/1365-2745.12477
- 605 Davies GM, Gray A (2015) Don't let spurious accusations of pseudoreplication limit our ability
606 to learn from natural experiments (and other messy kinds of ecological monitoring). *Ecol*
607 *Evol* 5:5295–5304. doi: 10.1002/ece3.1782
- 608 Diaz-Pulido G, Nash MC, Anthony KRN, Bender D, Opdyke BN, Reyes-Nivia C, Troitzsch U
609 (2014) Greenhouse conditions induce mineralogical changes and dolomite accumulation
610 in coralline algae on tropical reefs. *Nature Comm.* doi: 10.1038/ncomms4310
- 611 Donnarumma L, Lombardi C, Cocito S, Gambi MC (2014) Settlement pattern of *Posidonia*
612 *oceanica* epibionts along a gradient of ocean acidification : an approach with mimics.
613 *Mediterr Mar Sci* 15:498–509. doi: 10.12681/mms.677
- 614 Egilsdottir H, Noisette F, Noël LM-LJ, Olafsson J, Martin S (2013) Effects of pCO₂ on
615 physiology and skeletal mineralogy in a tidal pool coralline alga *Corallina elongata*. *Mar*
616 *Biol* 160:2103–2112. doi: 10.1007/s00227-012-2090-7
- 617 Fabry VJ, Seibel BA, Feely RA, Orr JC (2008) Impacts of ocean acidification on marine fauna
618 and ecosystem processes. *ICES J Mar Sci* 65:414–432. doi: 10.1093/icesjms/fsn048
- 619 Feely RA (2004) Impact of anthropogenic CO₂ on the CaCO₃ system in the oceans. *Science*
620 305:362–366. doi: 10.1126/science.1097329

- 621 Frankovich TA, Zieman JC (1994) Total epiphyte and epiphytic carbonate production on
622 *Thalassia testudinum* across Florida Bay. Bull Mar Sci 54:679–695.
- 623 Gattuso J-P, Kirkwood W, Barry JP, Cox TE, Gazeau F, Hansson L, Hendriks I, Kline DI,
624 Mahacek P, Martin S, McElhany P, Peltzer ET, Reeve J, Roberts D, Saderne V, Tait K,
625 Widdicombe S, Brewer PG (2014) Free-ocean CO₂ enrichment (FOCE) systems: present
626 status and future developments. Biogeosciences 11:4057–4075.
- 627 Gattuso J-P, Magnan A, Bille R, Cheung WWL, Howes EL, Joos F, Allemand D, Bopp L,
628 Cooley SR, Eakin CM, Hoegh-Guldberg O, Kelly RP, Portner H-O, Rogers AD, Baxter
629 JM, Laffoley D, Osborn D, Rankovic A, Rochette J, Sumaila UR, Treyer S, Turley C
630 (2015) Contrasting futures for ocean and society from different anthropogenic CO₂
631 emissions scenarios. Science 349:aac4722-aac4722. doi: 10.1126/science.aac4722
- 632 Gaylord B, Kroeker KJ, Sunday JM, Anderson KM, Barry JP, Brown NE, Connell SD, Dupont
633 S, Fabricius KE, Hall-Spencer JM, Klinger T, Milazzo M, Munday PL, Russell BD,
634 Sanford E, Schreiber SJ, Thiyagarajan V, Vaughan MLH, Widdicombe S, Harley CDG
635 (2015) Ocean acidification through the lens of ecological theory. Ecology 96:3–15. doi:
636 10.1890/14-0802.1
- 637 Gazeau F, Parker LM, Comeau S, Gattuso J-P, O'Connor WA, Martin S, Pörtner H-O, Ross PM
638 (2013) Impacts of ocean acidification on marine shelled molluscs. Mar Biol 160:2207–
639 2245. doi: 10.1007/s00227-013-2219-3
- 640 Gischler E, Dietrich S, Harris D, Webster JM, Ginsburg RN (2013) A comparative study of
641 modern carbonate mud in reefs and carbonate platforms: Mostly biogenic, some
642 precipitated. Sediment Geol 292:36–55. doi: 10.1016/j.sedgeo.2013.04.003
- 643 Gorsky G, Ohman MD, Picheral M, Gasparini S, Stemmann L, Romagnan JB, Cawood A,
644 Pesant S, Garcia-Comas C, Prejger F (2010) Digital zooplankton image analysis using
645 the ZooScan integrated system. J Plankton Res 32:285–303.
- 646 Hall-Spencer JM, Rodolfo-Metalpa R, Martin S, E, Fine M, Turner SM, Rowley SJ, Tedesco D,
647 Buia MC (2008) Volcanic carbon dioxide vents show ecosystem effects of ocean
648 acidification. Nature 454:96–99
- 649 Hemminga MA, Duarte CM (2000) Seagrass Ecology. University of Cambridge, Cambridge,
650 United Kingdom
- 651 Hendriks IE, Duarte CM, Olsen YS, Steckbauer A, Ramajo L, Moore TS, Trotter JA, McCulloch
652 M (2014a) Biological mechanisms supporting adaptation to ocean acidification in coastal
653 ecosystems. Estuar Coast Shelf Sci 152:1–8. doi: 10.1016/j.ecss.2014.07.019
- 654 Hendriks IE, Olsen YS, Ramajo L, Basso L, Steckbauer A, Moore TS, Howard J, Duarte CM
655 (2014b) Photosynthetic activity buffers ocean acidification in seagrass meadows.
656 Biogeosciences 11:333–346. doi: 10.5194/bg-11-333-2014

- 657 Hofmann LC, Bischof K (2014) Ocean acidification effects on calcifying macroalgae. *Aquat*
658 *Biol* 22:261–279
- 659 Hofmann LC, Koch M, de Beer D (2016) Biotic control of surface pH and evidence of light-
660 induced H⁺ pumping and Ca²⁺-H⁺ exchange in a tropical crustose coralline alga. *PLoS*
661 *ONE* 11: e0159057
- 662 Hurd CL (2015) Slow-flow habitats as refugia for coastal calcifiers from ocean acidification. *J*
663 *Phycol* 51:599–605. doi: 10.1111/jpy.12307
- 664 Hurlbert S (1984) Pseudoreplication and the design of ecological field experiments. *Ecol*
665 *Monogr* 187–211
- 666 Jackson EL, Rees SE, Wilding C, Attrill MJ (2015) Use of a seagrass residency index to
667 apportion commercial fishery landing values and recreation fisheries expenditure to
668 seagrass habitat service: Seagrass contribution to fishery value. *Cons Biol* 29:899–909.
669 doi: 10.1111/cobi.12436
- 670 Johnson MD, Moriarty VW, Carpenter RC (2014) Acclimatization of the crustose coralline alga
671 *Porolithon onkodes* to variable pCO₂. *PLoS ONE* 9:e87678. doi:
672 10.1371/journal.pone.0087678
- 673 Kerrison P, Hall-Spencer JM, Suggett DJ, Hepburn LJ, Steinke M (2011) Assessment of pH
674 variability at a coastal CO₂ vent for ocean acidification studies. *Estuar Coast Shelf Sci*
675 94:129–137
- 676 Keul N, Langer G, de Nooijer LJ, Bijma J (2013) Effect of ocean acidification on the benthic
677 foraminifera *Ammonia* sp. is caused by a decrease in carbonate ion concentration.
678 *Biogeosciences* 10:6185–6198. doi: 10.5194/bg-10-6185-2013
- 679 Kleypas J, Buddemeier R, Archer D, Gattuso J-P, Langdon C, Opdyke, B (1999) Geochemical
680 consequences of increased atmospheric carbon dioxide on coral reefs. *Science* 284:118–
681 120.
- 682 Koch M, Bowes G, Ross C, Zhang XH (2013) Climate change and ocean acidification effects on
683 seagrasses and marine macroalgae. *Glob Change Biol* 19:103–132. doi: 10.1111/j.1365-
684 2486.2012.02791.x
- 685 Kravesky-Self S, Richards JL, Rahmatian M, Fredericq S (2016) Aragonite infill in overgrown
686 conceptacles of coralline *Lithothamnion* spp. (Hapalidiaceae, Hapalidiales, Rhodophyta):
687 new insights in biomineralization and phylomineralogy. *J Phycol* 52:161–173. doi:
688 10.1111/jpy.12392
- 689 Kroeker KJ, Kordas RL, Crim R, Singh GG (2013) Impacts of ocean acidification on marine
690 organisms: quantifying sensitivities and interaction with warming. *Glob Change Biol*
691 19:1884–1896. doi: 10.1111/gcb.12179

- 692 Kroeker KJ, Kordas RL, Crim RN, Singh GG, Hendriks IE, Ramajo L, Singh GS, Duarte CM,
693 Gattuso J-P (2010) Meta-analysis reveals negative yet variable effects of ocean
694 acidification on marine organisms: Biological responses to ocean acidification. *Ecol Lett*
695 13:1419–1434. doi: 10.1111/j.1461-0248.2010.01518.x
- 696 Kroeker KJ, Micheli F, Gambi MC (2012) Ocean acidification causes ecosystem shifts via
697 altered competitive interactions. *Nat Clim Change* 3:156–159. doi: 10.1038/nclimate1680
- 698 Land LS (1970) Carbonate mud: production by epibiont growth on *Thalassia testudinum*. *J*
699 *Sediment Petrol* 40:1361–1363
- 700 Lepoint G, Havelange S, Gobert S, Bouquegneau JM (1999) Fauna vs flora contribution to the
701 leaf epiphytes biomass in a *Posidonia oceanica* seagrass bed (Revellata Bay, Corsica).
702 *Hydrobiologia* 394:63–67
- 703 Lepoint G, Jacquemart J, Bouquegneau JM, Demoulin V, Gobert S (2007) Field measurements
704 of inorganic nitrogen uptake by epiflora components of the seagrass *Posidonia oceanica*
705 (Monocotyledons, Posidoniaceae). *J Phycol* 43:208–218
- 706 Lepoint G, Nyssen F, Gobert S, Dauby P, Bouquegneau JM (2000) Relative impact of a seagrass
707 bed and its adjacent epilithic algal community in consumer diets. *Mar Biol* 136:513–518
- 708 Littler M, Littler D (2013) The nature of crustose coralline algae and their interactions on reefs.
709 *Smithson Contrib Mar Sci* 39:199–212
- 710 Lombardi C, Cocito S, Gambi M, Cisterna B, Flach F, Taylor P, Keltie K, Freer A, Cusack M
711 (2011a) Effects of ocean acidification on growth, organic tissue and protein profile of the
712 Mediterranean -bryozoan *Myriapora truncata*. *Aquat Biol* 13:251–262. doi:
713 10.3354/ab00376
- 714 Lombardi C, Gambi MC, Vasapollo C, Taylor P, Cocito S (2011b) Skeletal alterations and
715 polymorphism in a Mediterranean bryozoan at natural CO₂ vents. *Zoomorphology*
716 130:135–145. doi: 10.1007/s00435-011-0127-y
- 717 Mabrouk L, Ben Brahim M, Hamza A, Mahfoudhi M, Bradai MN (2014) A comparison of
718 abundance and diversity of epiphytic microalgal assemblages on the leaves of the
719 seagrasses *Posidonia oceanica* (L.) and *Cymodocea nodosa* (Ucria) Asch in Eastern
720 Tunisia. *J Mar Biol* 2014:1–10. doi: 10.1155/2014/275305
- 721 Martin S, Gattuso J-P (2009) Response of Mediterranean coralline algae to ocean acidification
722 and elevated temperature. *Glob Change Biol* 15:2089–2100. doi: 10.1111/j.1365-
723 2486.2009.01874.x
- 724 Martin S, Rodolfo-Metalpa R, Ransome E, Rowley S, Buia M-CC, Gattuso J-P, Hall-Spencer J
725 (2008) Effects of naturally acidified seawater on seagrass calcareous epibionts. *Biol Lett*
726 4:689–692. doi: 10.1098/rsbl.2008.0412

- 727 Martínez-Crego B, Olivé I, Santos R (2014) CO₂ and nutrient-driven changes across multiple
728 levels of organization in *Zostera noltii* ecosystems. *Biogeosciences* 11:7237–7249
- 729 McCoy SJ, Kamenos NA (2015) Coralline algae (Rhodophyta) in a changing world: integrating
730 ecological, physiological, and geochemical responses to global change. *J Phycol* 51:6–24
731 doi: 10.1111/jpy.12262
- 732 McCoy SJ, Ragazzola F (2014) Skeletal trade-offs in coralline algae in response to ocean
733 acidification. *Nat Clim Change* 4:719–723. doi: 10.1038/nclimate2273
- 734 Nash MC, Opdyke BN, Wu Z, Xu H, Trafford JM (2014) Simple X-Ray diffraction techniques
735 to identify Mg-calcite, dolomite, and magnesite in tropical coralline algae and assess peak
736 asymmetry. *J Sediment Res* 83:1084–1098. doi: 10.2110/jsr.2013.67
- 737 Nash MC, Troitzsch U, Opdyke BN, Trafford JM, Russell BD, Kline DI (2011) First discovery
738 of dolomite and magnesite in living coralline algae and its geobiological implications.
739 *Biogeosciences* 8:3331–3340. doi: 10.5194/bg-8-3331-2011
- 740 Nelsen JE, Ginsburg RN (1986) Calcium carbonate production by epibionts on *Thalassia* in
741 Florida Bay. *J Sediment Res Vol.* 56:622–628. doi: 10.1306/212F89EF-2B24-11D7-
742 8648000102C1865D
- 743 Nelson W (2009) Calcified macroalgae—critical to coastal ecosystems and vulnerable to change:
744 a review. *Mar Freshwater Res* 60:787–801. doi: 10.1071/MF08335
- 745 Oksanen L (2001) Logic of experiments in ecology: is pseudoreplication a pseudoissue? *Oikos*
746 94:27–38. doi: 10.1034/j.1600-0706.2001.11311.x
- 747 Pasqualini V, Pergent-Martini C, Clabaut P, Pergent G (1998) Mapping of *Posidonia oceanica*
748 using aerial photographs and side scan sonar: application off the island of Corsica
749 (France). *Estuar Coast Shelf Sci* 47:359–367
- 750 Perry CT, Beavington-Penney SJ (2005) Epiphytic calcium carbonate production and facies
751 development within sub-tropical seagrass beds, Inhaca Island, Mozambique. *Sediment*
752 *Geol* 174:161–176. doi: 10.1016/j.sedgeo.2004.12.003
- 753 Pettit LR, Smart CW, Hart MB, Milazzo M, Hall-Spencer JM (2015) Seaweed fails to prevent
754 ocean acidification impact on foraminifera along a shallow-water CO₂ gradient. *Ecol*
755 *Evol* 5:1784–1793. doi: 10.1002/ece3.1475
- 756 Pinckney JL, Fiorenza M (1998) Microalgae on seagrass mimics: Does epiphyte community
757 structure differ from live seagrasses? *J Exp Mar Biol Ecol* 221:59–70
- 758 Prado P, Alcoverro T, Romero J (2008) Seasonal response of *Posidonia oceanica* epiphyte
759 assemblages to nutrient increase. *Mar Ecol Prog Ser* 359:89–98

- 760 Rodolfo-Metalpa R, Lombardi C, Cocito S, Hall-Spencer JM, Gambi MC (2010) Effects of
761 ocean acidification and high temperatures on the bryozoan *Myriapora truncata* at natural
762 CO₂ vents. *Mar Ecol* 31:447–456. doi: 10.1111/j.1439-0485.2009.00354.x
- 763 Roleda MY, Cornwall CE, Feng Y, McGraw CM, Smith AM, Hurd CL (2015) Effect of ocean
764 acidification and pH Fluctuations on the growth and development of coralline algal
765 recruits, and an associated benthic algal assemblage. *PLOS ONE* 10:e0140394. doi:
766 10.1371/journal.pone.0140394
- 767 Saderne V, Wahl M (2013) Differential responses of calcifying and non- calcifying epibionts of
768 a brown macroalga to present-day and future upwelling pCO₂. *PLoS ONE* 8:e70455. doi:
769 10.1371/journal.pone.0070455
- 770 Small DP, Milazzo M, Bertolini C, Graham H, Hauton C, Hall-Spencer JM, Rastrick SPS (2016)
771 Temporal fluctuations in seawater p CO₂ may be as important as mean differences when
772 determining physiological sensitivity in natural systems. *ICES J Mar Sci* 73:604–612.
773 doi: 10.1093/icesjms/fsv232
- 774 Smith AM (2014) Growth and calcification of marine bryozoans in a changing ocean. *Biol Bull*
775 226:203–210
- 776 Smith AM, Sutherland JE, Kregting L, Farr TJ, Winter DJ (2012) Phylomineralogy of the
777 coralline red algae: Correlation of skeletal mineralogy with molecular phylogeny.
778 *Phytochemistry* 81:97–108. doi: 10.1016/j.phytochem.2012.06.003
- 779 Steel JB, Wilson BJ (2003) Which is the phyte in epiphyte? *Folia Geobotanica* 38:97–99. doi:
780 10.1007/BF02803129
- 781 Stewart-Oaten A, Murdoch W, Parker K (1986) Environmental impact assessment:
782 “Pseudoreplication” in time? *Ecol* 67:929–940
- 783 Sunday JM, Fabricius KE, Kroeker KJ, Anderson KM, Brown NE, Barry JP, Connell SD,
784 Dupont S, Gaylord B, Hall-Spencer JM, Klinger T, Milazzo M, Munday PL, Russell BD,
785 Sanford E, Thiyagarajan V, Vaughan MLH, Widdicombe S, Harley CDG (2016) Ocean
786 acidification can mediate biodiversity shifts by changing biogenic habitat. *Nat Clim*
787 *Change* 7:81–85. doi: 10.1038/nclimate3161
- 788 Tomas F, Turon X, Romero J (2005) Effects of herbivores on a *Posidonia oceanica* seagrass
789 meadow: importance of epiphytes. *Mar Ecol Prog Ser* 287:115–125
- 790 Vizzini S, Di Leonardo R, Costa V, Tramati CD, Luzzu F, Mazzola A (2013) Trace element bias
791 in the use of CO₂ vents as analogues for low pH environments: implications for
792 contamination levels in acidified oceans. *Estuar Coast Shelf Sci* 134:19–30. doi:
793 10.1016/j.ecss.2013.09.015

Figure captions

Fig. 1 nMDS based upon the Bray-Curtis Index of dissimilarity for the epiphytic community within the reference plot, control and experimental enclosure (represented by symbols) at each sampling interval, labeled 1 to 4 for T1 to T4 which corresponds to 0, 39, 74, 109, 135 d after the pH manipulation in the months of June, July, September, October and November respectively

Fig. 2 A - G are boxplots showing the minimum, maximum, mean (dotted line) and median (solid line) coverage (%) of each epiphytic taxonomic or functional unit as occurred on leaves (N = 3 to 7) collected from the ambient (sampled 1x, T0), reference plot (ambient environment, T1 to T4) and two enclosures (control and experimental) at sampling intervals T0 to T4 (intervals correspond to 0, 39, 74, 109, 135 d after the pH manipulation in the months of June, July, September, October and November, respectively)

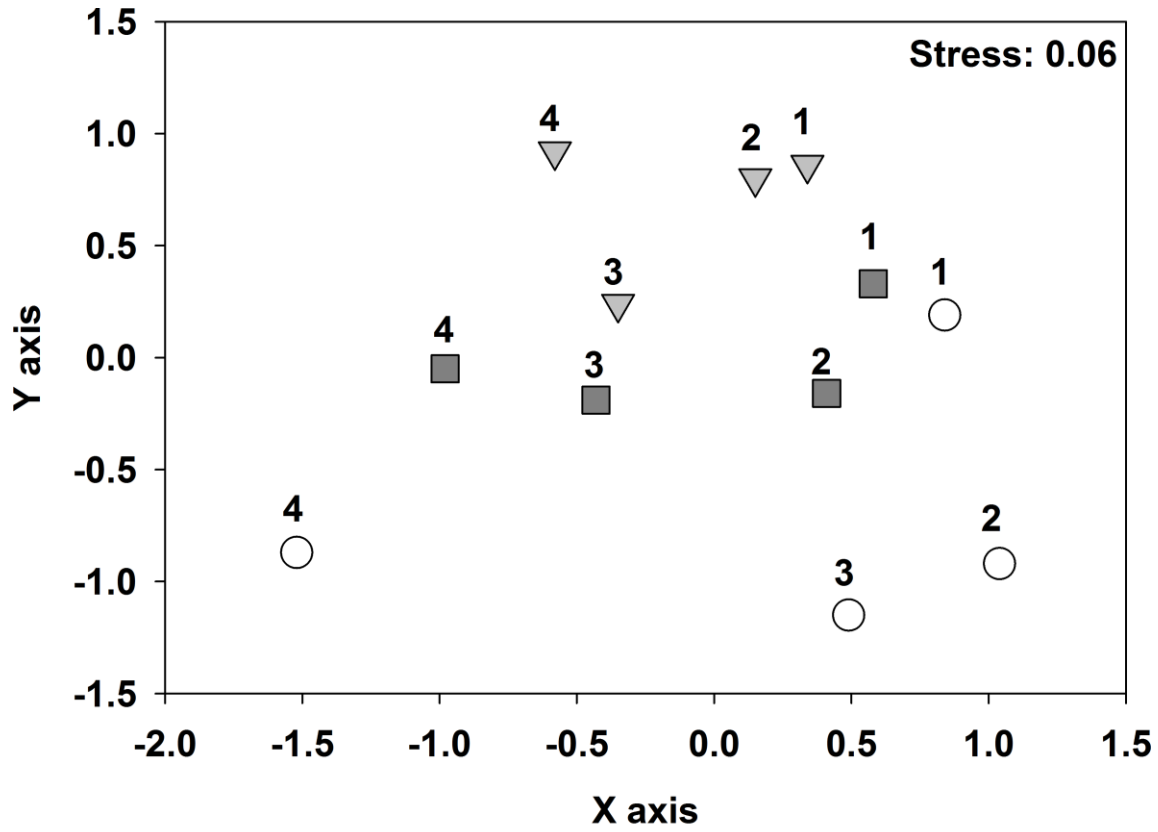
Fig. 3 Boxplots showing the minimum, maximum, mean (dotted line) and median (solid line) epiphytic total and calcareous organism coverage (%) as well as calcium carbonate (CaCO₃) mass (mg cm⁻², N = 3 to 7 leaves) in the ambient (sampled 1x, T0), reference plot (ambient environment, T1 to T4) and two enclosures (control and experimental) at sampling intervals T0 to T4 (See Fig.1 for additional details on intervals)

Fig. 4 Results from XRD with principles of peak asymmetry show, for each sample, the mol % magnesium in carbonate for the bulk epiphytes in the ambient (location sampled

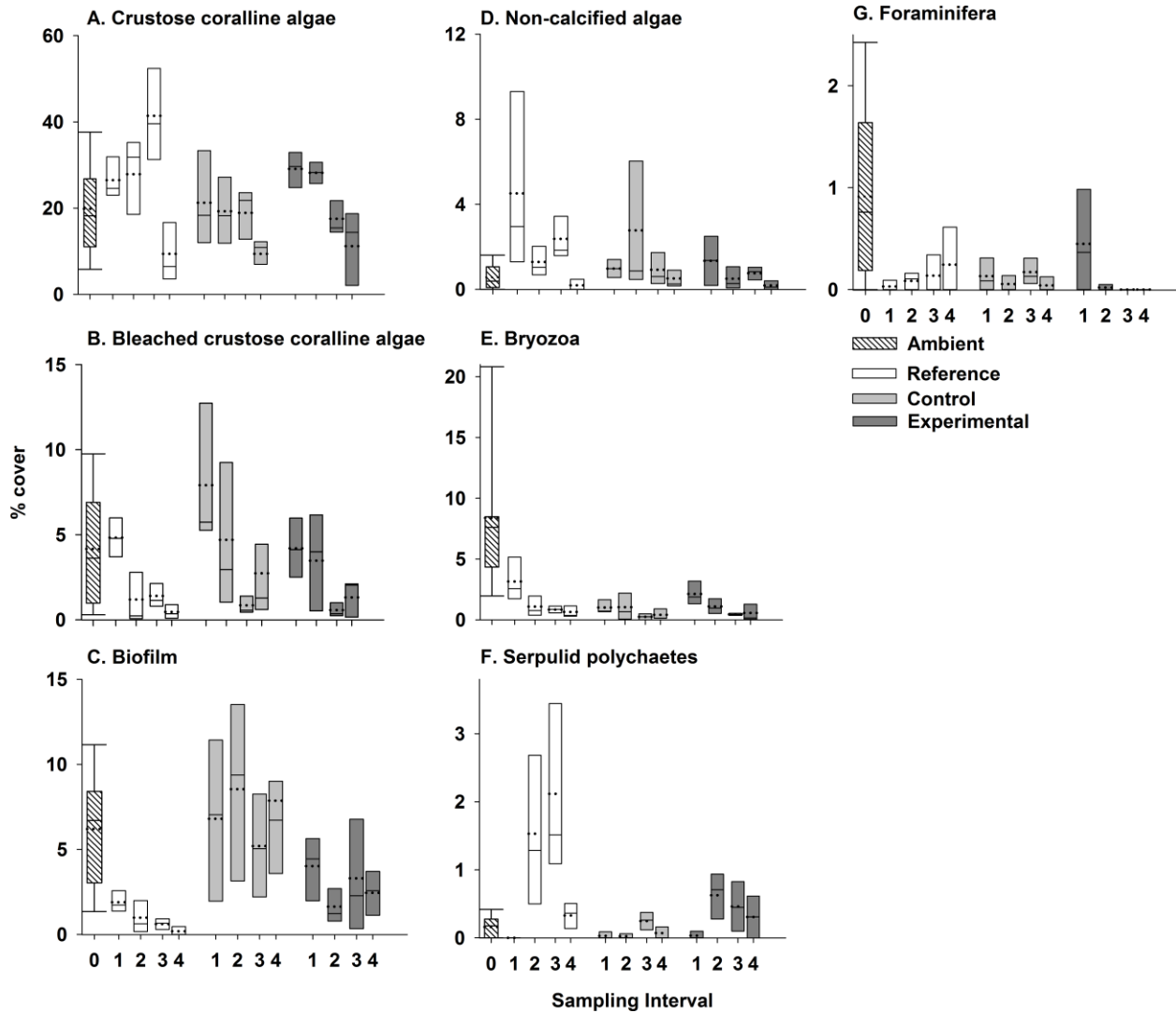
1x, T0), reference plot (ambient environment, T1 to T4) and two enclosures (control and experimental) at sampling intervals T0 to T4 (N = 3 leaves, see Fig. 1 for additional details on intervals). The relative calcite asymmetry is shown in panel B; values were not quantified. Aragonite (C) was determined from the area under the curve

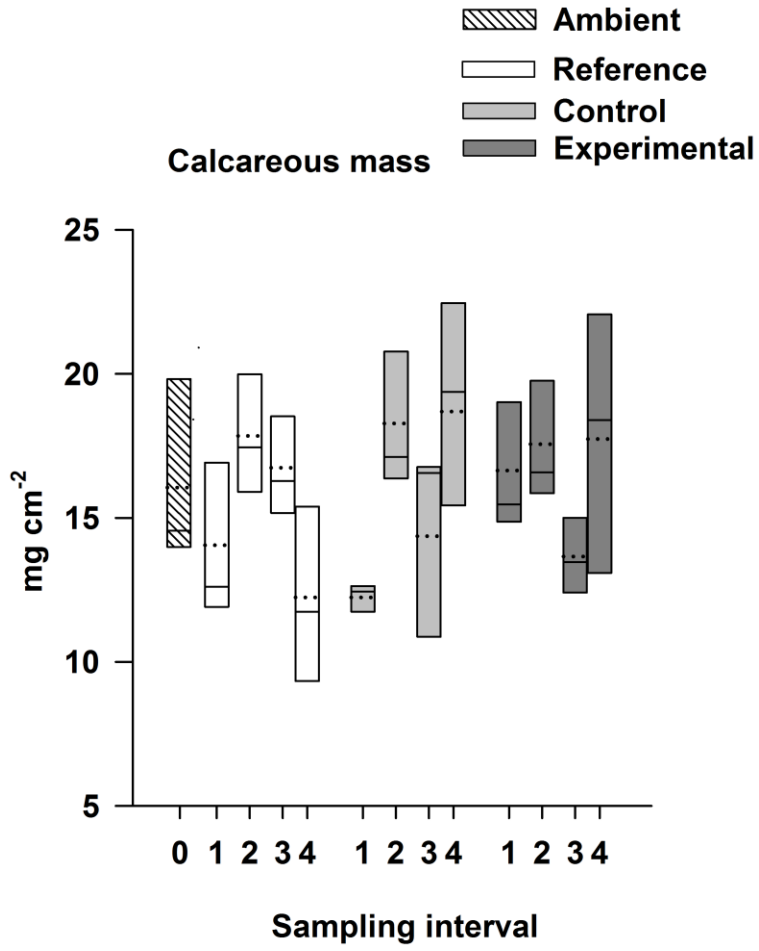
Fig. 5 SEM-EDS images of typical cell wall calcification of epiphytic crustose coralline algae (CCA) as observed in enclosures (control and pH-manipulated experimental) and ambient environment (T0 and reference plot) throughout the duration of study. Images A and B show crustose coralline algae on the leaf. B is a closer view of the outlined area where Mg-calcite (Mg-C) grains were observed. C and D show the crustose coralline cell walls and interfilaments engrained with Mg-calcite crystals

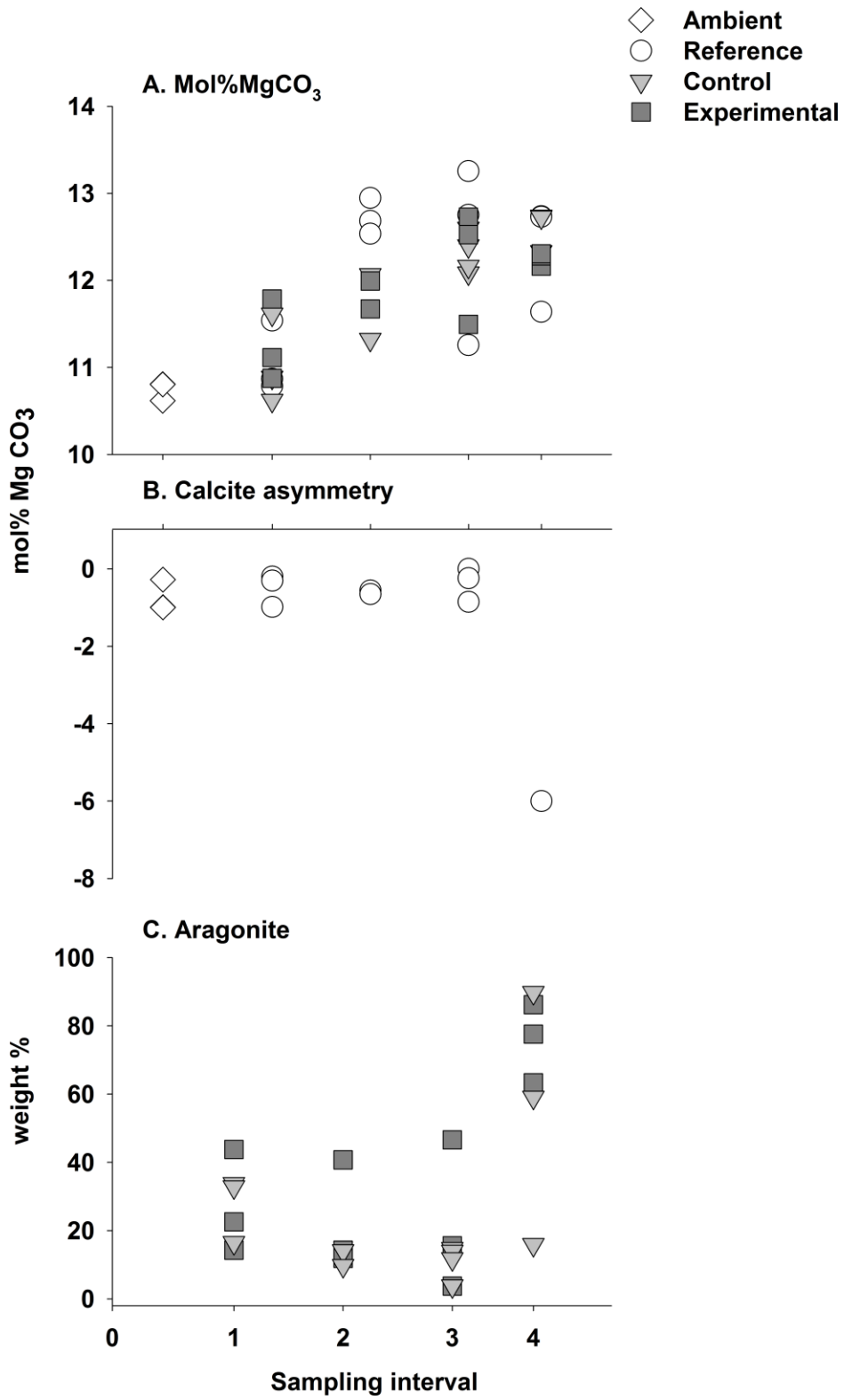
Fig. 6 SEM-EDS images of alteration of mineral composition in epiphytic crustose coralline algae as occurred on leaves from the ambient environment (T0 and reference plot) and two enclosures (control and pH-manipulated experimental). A-C (left) demonstrate mineral alteration between Mg-calcite (Mg-C) and calcite (abbreviated as C) which occurred in the ambient environment. A shows the location of calcite (white outline) and Mg-calcite. In closer view of the altered area (B and C) calcite grains can be observed. D-E demonstrates alteration from Mg-calcite to aragonite which occurred in the enclosures. D is an image of crustose coralline algae on the leaf surface showing altered patches where aragonite occurred; in closer view (E and F) the altered surfaces lacked cell wall features and clear crystal shape

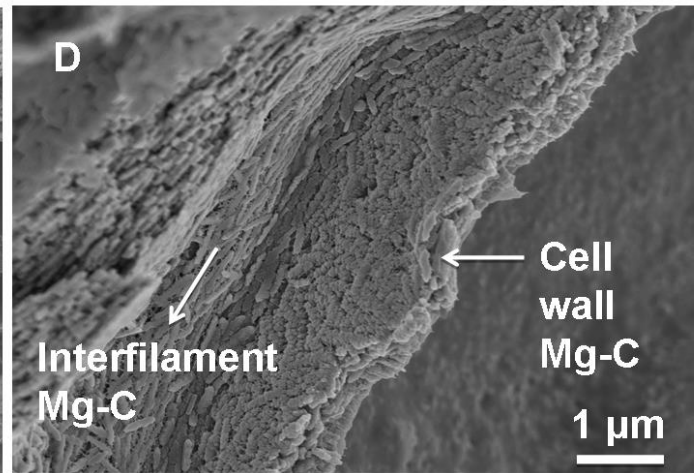
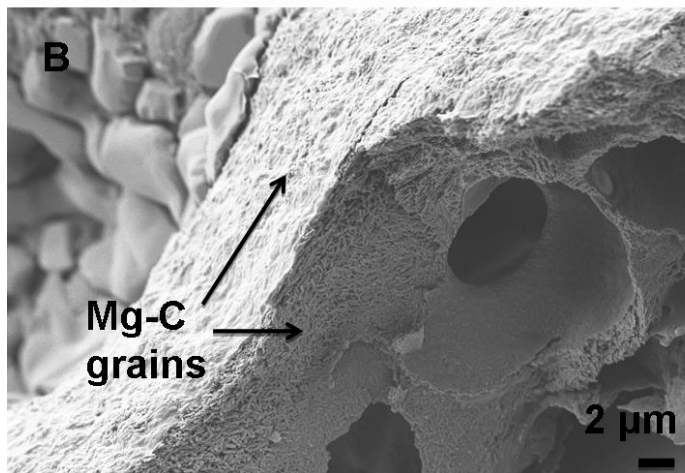
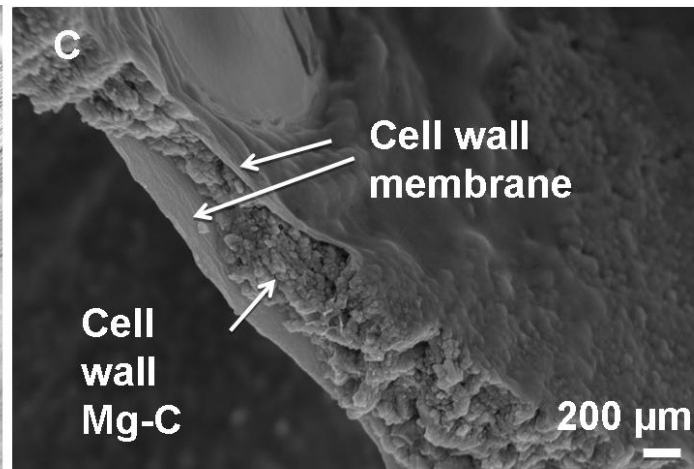
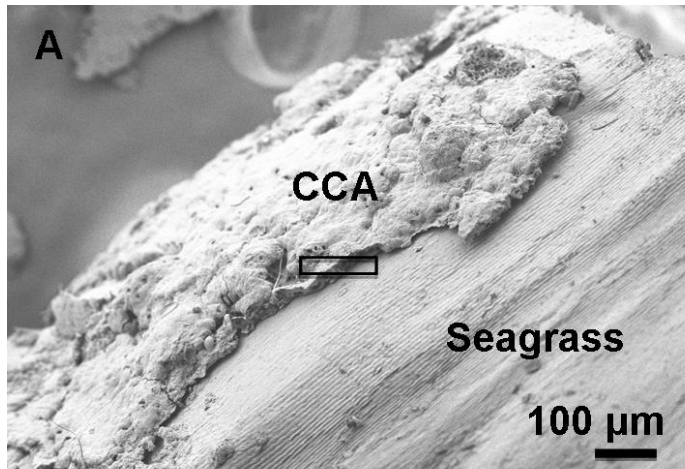


- Reference
- ▽ Control
- Experimental









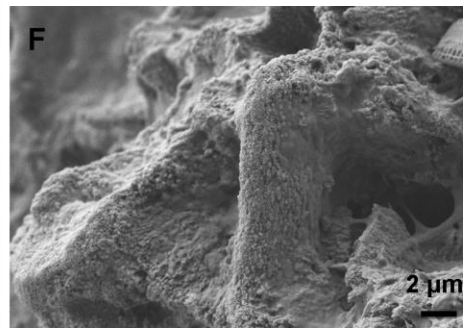
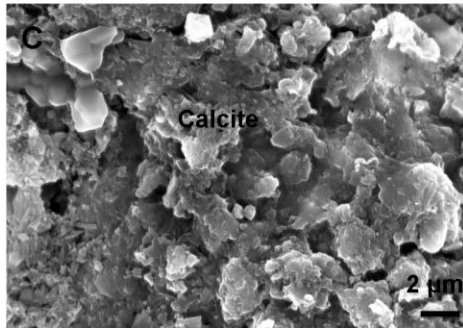
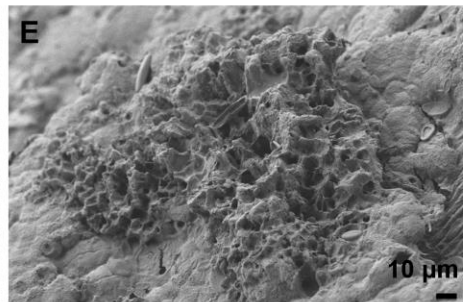
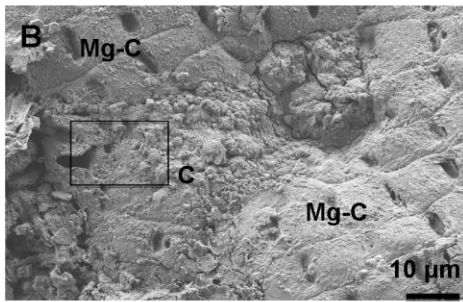
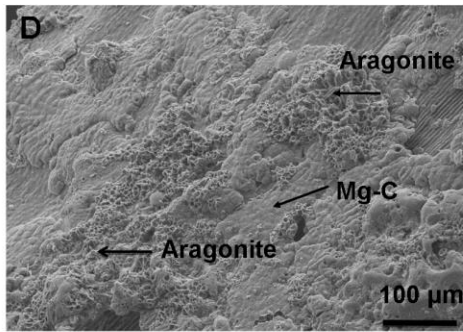
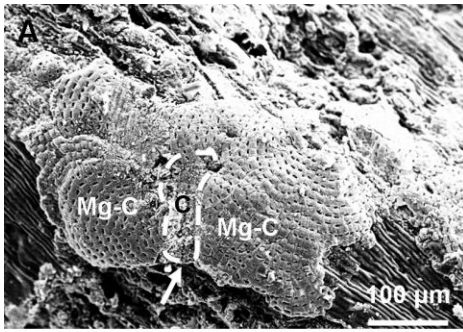


Table 1. Carbonate chemistry within ambient and enclosures: mean (\pm standard deviation, SD) pH (on the total scale; pH_T), partial pressure of carbon dioxide ($p\text{CO}_2$) and saturation states with respect to aragonite (Ω_a) and calcite (Ω_c) for each month and the period before and during acidification. The difference in pH_T between the experimental and the control enclosure is also shown (Diff)

Period Months	N Samples	pH _T								$p\text{CO}_2$ (μatm)						Ω_a			Ω_c								
		Ambient		Control		Experimental		Diff		Ambient		Control		Experimental		Ambient		Control		Experimental							
		Mean	SD	Mean	SD	Mean	SD	Mean	SD	Mean	SD	Mean	SD	Mean	SD	Mean	SD	Mean	SD	Mean	SD	Mean	SD	Mean	SD		
<i>Before</i>																											
May	11840	8.10	0.03	8.12	0.06	8.01	0.05	-0.10	0.03	374	30	358	55	477	74	3.4	0.2	3.5	0.4	2.9	0.3	5.3	0.3	5.4	0.5	4.5	0.5
June	8119	8.11	0.04	8.04	0.05	8.10	0.06	0.06	0.05	369	38	443	63	378	65	3.5	0.3	3.1	0.4	3.5	0.4	5.4	0.4	4.8	0.5	5.4	0.5
<i>Acidification</i>																											
June	6226	8.05	0.03	8.02	0.04	7.79	0.13	-0.23	0.13	430	42	470	57	868	318	3.6	0.2	3.3	0.3	2.3	0.6	5.4	0.4	5.1	0.4	3.5	0.9
July	21007	8.03	0.03	8.03	0.06	7.79	0.12	-0.24	0.11	454	46	453	81	870	254	3.6	0.2	3.6	0.4	2.4	0.6	5.4	0.4	5.4	0.6	3.6	0.8
August	22682	8.00	0.03	8.04	0.07	7.81	0.12	-0.23	0.09	489	42	445	85	834	253	3.5	0.2	3.7	0.5	2.5	0.6	5.3	0.3	5.7	0.7	3.8	0.9
September	21854	7.98	0.07	7.97	0.06	7.70	0.11	-0.27	0.10	521	96	536	87	1098	288	3.3	0.4	3.2	0.3	2.0	0.5	5.0	0.6	4.9	0.5	3.0	0.7
October	22420	8.01	0.04	8.00	0.04	7.70	0.13	-0.29	0.14	480	52	497	64	1086	390	3.4	0.2	3.3	0.3	2.0	0.5	5.1	0.4	5.0	0.4	3.0	0.8
November	5377	8.02	0.03	8.02	0.02	7.80	0.15	-0.22	0.15	469	48	467	22	836	305	3.2	0.2	3.2	0.1	2.2	0.7	4.9	0.3	4.9	0.2	3.5	1.0
Before	24334	8.10	0.04	8.05	0.07	8.06	0.07	0.01	0.09	380	39	434	85	426	87	3.5	0.2	3.2	0.4	3.3	0.5	5.4	0.4	4.9	0.6	5.0	0.7
Acidification	95711	8.01	0.05	8.01	0.06	7.75	0.13	-0.26	0.11	483	67	482	86	971	323	3.4	0.3	3.4	0.4	2.2	0.6	5.2	0.4	5.2	0.6	3.6	0.9